Makara Journal of Science

Volume 17 | Issue 1 Article 4

4-25-2013

Determining the Source Parameters of the Jambi Earthquake (1 October 2009, Mw=6.4) Using Three-Component Local Waveforms

Madlazim Madlazim
Department of Physics, Faculty of Mathematics and Natural Sciences, Universitas Negeri Surabaya, Surabaya 60231, Indonesia, m_lazim@fisika.fmipa.unesa.ac.id

Makara Journal of Science 17/1 (2013) 17-22

Determining the Source Parameters of the Jambi Earthquake (1 October 2009, M_w=6.4) Using Three-Component Local Waveforms

Madlazim

Department of Physics, Faculty of Mathematics and Natural Sciences, Universitas Negeri Surabaya, Surabaya 60231, Indonesia

E-mail: m_lazim@fisika.fmipa.unesa.ac.id

Abstract

The purpose of this research was to estimate the source parameters of a mainshock earthquake (Mw=6.4) that occurred on 1 October 2009 in the Dikit major segment of the Sumatran Fault Zone (SFZ). The source parameters were analyzed by the inversion of three-component local waveforms recorded by the GEOFON broadband IA network. Moment tensor of the event was determined using the Discrete Wave number method to calculate the Green function and the iterative deconvolution method to invert the moment tensors. From the analysis, we obtained the fault parameters of the mainshock, which are strike=324°, dip= 80° and rake= -173°.

Abstrak

Penentuan Parameter Sumber Gempabumi Jambi (1 Oktober 2009, M_w=6,4) Menggunakan Tiga Komponen *Waveforms* Lokal. Penelitian ini bertujuan untuk mengestimasi parameter sumber gempa bumi utama (Mw-6,4) yang terjadi pada 1 Oktober 2009 di segmen Dikit yang merupakan bagian dari *Sumatra Fault Zone* (SFZ). Parameter sumber gempa bumi dianalisis menggunakan metode inversi tiga komponen *waveform* lokal yang direkam oleh jaringan stasiun seismik GEOFON-IA. Momen tensor dari gempa bumi ditentukan dengan metode *discrete wavenumber* untuk menghitung fungsi *Green*. Selanjutnya momen tensor ditentukan menggunakan metode dekonvulasi untuk menginversi momen tensor. Berdasarkan hasil analisis ditemukan bahwa tipe sesar yang menyebabkan gempa bumi utama memiliki *strike*=324°, dip= 80° dan *rake*= -173°.

Keywords: discrete wavenumber method, earthquake local waveform, inversion method

1. Introduction

The mainshock event 20091001_01:52:27.77 (with moment magnitude Mw=6.4, hypocenter (lat.=-2.603°; lon.=101.511° and depth=10.0 km) occurred at the Dikit segment of the Sumatra Fault Zone (SFZ).The length of the segment is 60 km with a latitude of -2.75° to -2.30° [1]. Twelve aftershocks occurred on the segment. (These events can be accessed at BMKG-net at http://www.bmg.go.id and GEOFON-net at http://geofon.gfz-potsdam.de/geofon/new/netabs/ia req. html.). In this study, we focus on the Dikit segment. Aftershocks usually occur geographically near the main shock. The stress on the main shock's fault drastically changes during the main shock and that fault produces most of the aftershocks. Occasionally, the change in stress caused by the main shock is great enough to trigger aftershocks on other, nearby faults, and for a very large main shock, sometimes even further away. As a rule, we call events aftershocks if they are at a distance from the main shock fault no greater than the length of that fault of the segment.

In this paper, we present three-component local waveforms that were recorded by eight GEOFON and IA network stations (Figure 1). The epicentral distances of all stations were less than 516 km. The stations provide good azimuthal coverage and the data quality is good. We analyzed the three-component local waveforms to predict the source parameters of the main shock.

There are two zones in Sumatra where earthquakes occur frequently: (1) the subduction zone located in the West Sumatran ocean, which has the power to cause earthquakes of a relatively large magnitude, thus creating a significant chance of tsunamis, and (2) the SFZ, also known as the Semangko fault. The Semangko fault separates Sumatra Island into two parts, spreading out along the Bukit Barisan mountain range, from Semangko Bay in Sunda Strait to Aceh in the north. It is a very active fault. The earthquakes that occur in Java and Sumatra are a geodynamic implication of an active deformation around Sunda (Java) Trench [3].

Most of the strike-slip components of the oblique convergence between the Indian–Australian plate and the Eurasian plate southwest of Sumatra are accommodated by a right-lateral slip along the trench-parallel Sumatran fault, lying roughly 250 km northeast of the trench [1]. Therefore, the slip along the subduction zone itself has relatively small strike-parallel components.

Many giant earthquakes ($M_w \geq 8{:}0$) have occurred along the Sumatran mega thrust in the last 250 years, releasing the strain accumulated by the convergence between the two tectonic plates [2]. The earliest of these historical events was in February 1797 [4]. The earthquake had an Mw of 8.7 and ruptured the 370 km segment from 1° S to about 4° S [1]. This was followed by the giant earthquakes of 1833 (Mw=9.0), which ruptured a 500-km-long segment south of Siberut Island, and 1861 (Mw=8.5), which ruptured a 270-km-long segment beneath Nias Island [4]. After1861, no earthquake with an Mw≥8:0 occurred along the Sumatran megathrust until 26 December 2004, when the M_w=9.3 Aceh-Andaman earthquake happened [5].

Padang and Bengkulu, including the Dikit segment, are two major cities located along the high-seismicity region of the western coast of Sumatra. They are situated in the vicinity of the active, right-lateral Sumatran fault [1] and are also close to the Sumatran megathrust. Bengkulu is located in seismic zone 6, while Padang is in zone 5 [5].

2. Methods

This study focuses on the source parameters of the Jambi mainshock event that occurred on 1 October 2009. The earthquake's characteristics can be determined by the source parameters obtained by analyzing earthquake data known as seismic waves. The seismic wave propagated from the earthquake source (hypocenter) is recorded by the observatory stations installed around the earthquake region. To obtain the seismic wave of this particular earthquake, we used three-component local waveforms recorded by eight GEOFON and IA network stations (PDSI, RGRI, LHSI, MDSI, LWLI, KASI, PPBI and BLSI) installed around the epicenter of the main shock (Fig. 1). The epicentral distances of the stations are 217 km, 257.48 km, 261 km, 363 km, 391 km, 465 km, 512 km and 516 km, respectively. The distances are compatible with the ISOLA software for local data (epicentral distances ≤1000 km).

Before the full waveforms were used as input data to invert the moment tensors—the waveforms of the main shock were processed using seismic analysis code (SAC) software [6] the instrumental correction was first performed on the selected seismograms. Before applying the instrumental correction, the trend and mean were removed from the traces. However, the instrumental corrections on the broadband seismograms were applied using the built-in facility of the ISOLA (Isolated Asperity) software [7]. Finally, the corrected velocity traces were cut from the origin time to 250 s and they were filtered between 0.01 and 9.0 Hz using four pole band-pass Butterworth filters, using SAC. The input of the ISOLA code is derived from the band-passed velocity records, which are later integrated into the band-passed displacement traces inside ISOLA. These displacement traces were used as input data for the full waveform moment tensor inversion built-in, in the ISOLA software. The three-component seismograms of the mainshock recorded by the GEOFON network were inverted using the Green function that is calculated iteratively using the discrete-wave number method [8]. To calculate the Green function, we used a 1-D velocity model [9] and the hypocenter of the event taken from GEOFON.

We examined four velocity models in Sumatra (Combined Haslinger, Haslinger, Tselentis, and Novotny) using HIPOINVERSE software, and obtained the Combined Santosa and Haslinge velocity model that has the best rms and variance reduction [9]. This velocity model is a research result of Madlazim *et al*. [9], which we verified and modified to implement in the Sumatra research. The first six layers of all the velocity models with their parameters were determined using Haslinger *et al*. [10] as a reference. The seventh layer, along with all of its parameters, is a verified and modified result of our own research.

The next step involves theinversion ofthe three-component waveforms using the iteration deconvolution method [11]. This method was implemented in the ISOLA software [12] as a numerical simulation program development [13] to obtain the earthquake's source parameters. The inversion uses a frequency band between 30 MHz and75 MHz. The moment tensors of the mainshock event on 1 October 2009 were calculated using the waveform inversion of the three-component local broadband records of the GEOFON-IA network. The network belongs to the GFZ German Research Centre for Geosciences. More details on and present status of the network and its stations can be found at the Centre's website at http://www.webdc.eu. We calculated the moment tensors of the 1 October 2009 event using a 1-D crustal velocity model [9], the stations (Fig. 1) and frequency range of 30–75 mHz. The different filters mean different signal-to-noise ratios, related to smaller magnitudes and different locations and depths. Alow frequency is preferred because in this case the modeling is less (inherently) dependent on the structure of the earth's crust.

The ISOLA software was used for this research, combining the computational speed of Fortran and the user-friendly features of Matlab [7]. This method makes use of the inverse-problem formulation [12] based on six elementary MT components. Their equation is used to quickly evaluate the correlation between observed and synthetic waveforms. The Green functions are calculated using the discrete-wave number method [7-8]. The match between the observed and best-fitting synthetic data is characterized by the overall variance reduction: var. red. =1-E/O, where $E=\Sigma(O_i - S_i)^2$, $O=\Sigma(O_i)^2$, with O and S standing for the observed and synthetic data, along with the summation of all samples, components, and stations. The code also allows for complex rupture histories described by multiple point-source sub-events, each one represented by a delta function [12]. The three-component waveform inversion was conducted using the iterative deconvolution method [7,13] for regional distances, implemented in the ISOLA software. Complete waveforms were used without any separation of the body and surface waves. Waveform data processing is made easy using the Fortran Matlab ISOLA_GUI package program. The code facilitates the use of a multi-source-point model. In this study, we used single-source and deviatorical inversion (without any volume changes). Deviatorical tensor decomposition commonly consists of two components: a double-couple (DC) part and a compensated linear vector dipole (CLVD) part as a (non-DC) component. In this study, both components were determined. However, the benefit of the non-DC component as a physical parameter of tectonic earthquakes is exceedingly limited because the available crustal model is only an approximation [14].

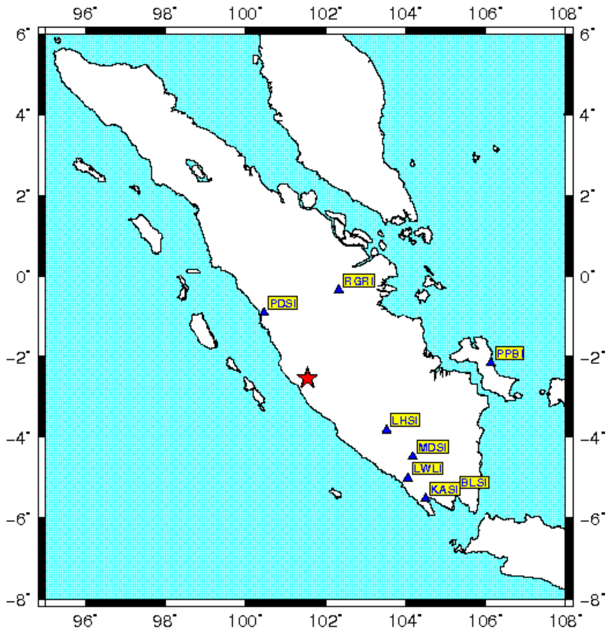

Figure 1. Epicenter of the Mainshock, 01-10-2009 Event (Red Star), Stations Distribution (Blue Triangles)

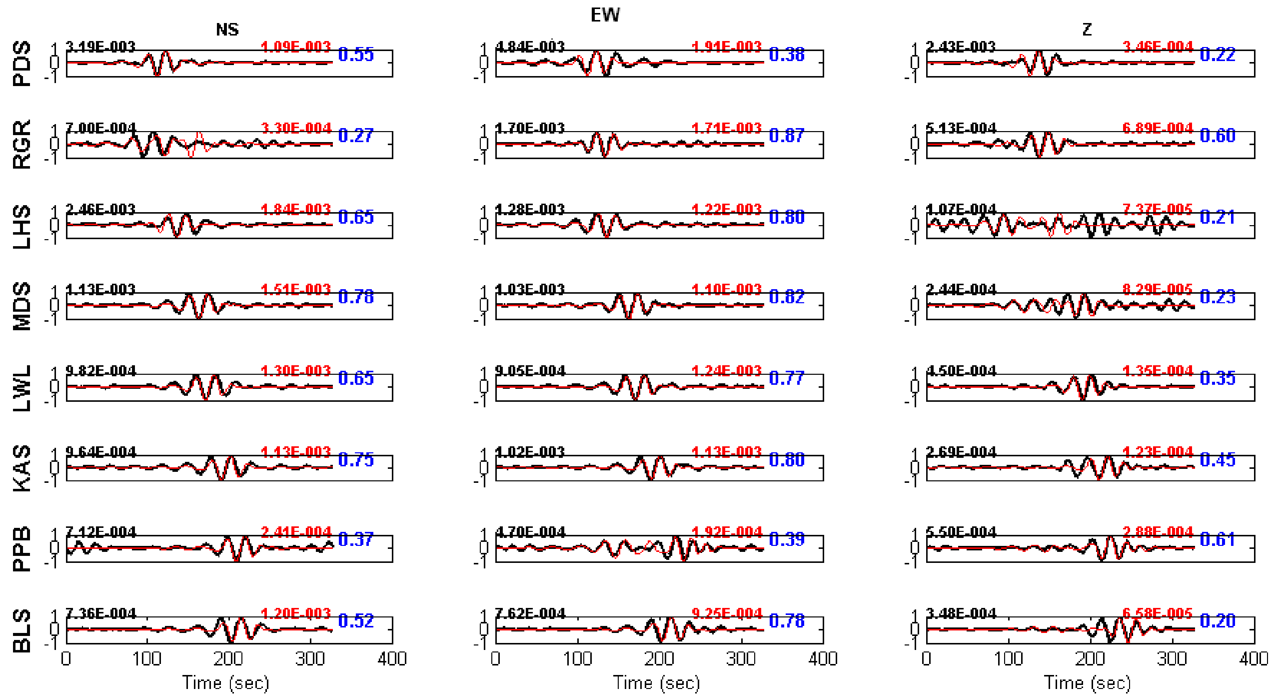

Figure 2. Observed Three-Component Local Waveforms of the Mainshock (Black), Synthetic (Red), and Blue Numbers are Variance Reduction for the Mainshock

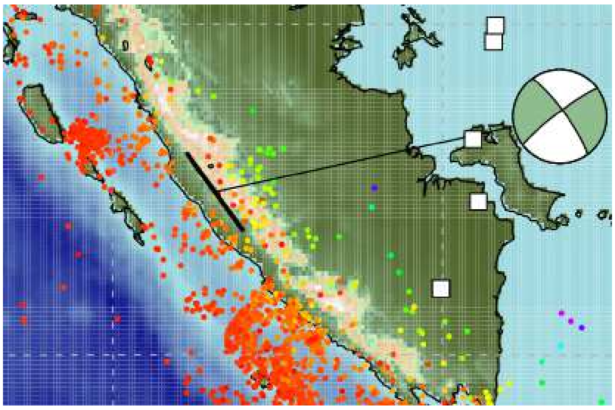

Figure 3. Centroid Moment Tensor and Centroid Epicenter and Strike Line of the 1 October 2009 Event

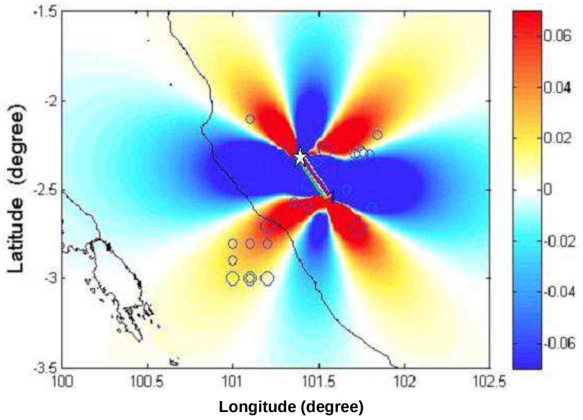

Figure 4. Increasing Coulomb Stress of the 1 October 2009 Event and Seismicity from 5 to 27 km Depth. Black Circles Indicate Seismicity, White Stars Indicate the Mainshock, and Rectangles Indicate the Activated Fault Plane Model

Table 1. Centroid Numerical Solution of the Event

Event	Lat	Long	Depth	Str1:str2	Dip1:Dip2	Rake1:Rake2	Mw	CT (s)
2009/10/0101:52	-2.54	101.55	12.0	235; 324	87; 80	-18; -173	6.4	6.16

An estimate of the source position is required to calculate the moment tensors. Here we distinguish between hypocenter and centroid moment tensors.

Centroid moment tensors represent the center of moment release in the faulted area. The centroid can be determined during the retrieval of the moment tensors as a point that will optimize the waveform fit, found by a grid search around an assumed position. Analogously, a temporal grid search provides the centroid time. For large events, the hypocenter and centroid do not coincide with each other. The moment tensor calculations for the event were completed using optimum source positions and time grid-search in three stages using the ISOLA software [7]. First, we used a 25-point grid stencil centered below the GEOFON epicenters with depths of 5, 10, 15, and 20 km, with 10 km increments both in the NS and EW directions. At each depth, the moment tensor corresponding to the optimum time is highly variable with the trial spatial positions, where the correlation has its maximum value. Second, we computed the moment tensors along a vertical line passing through the optimum position in the previous stage. Third, fixing the optimum depth of the optimum position, we focused on the spatial-temporal search. Figure 4 shows the waveform fit for the moment tensor solution of event 01-10-2009_01:52:27.77, with M_w=6.4; the red waveform is the synthetic, the black is the observed. Seismic moment (M_0), magnitude moment (M_w), depth, orientation, fault plane width, and slip length were determined for the event. As afore mentioned, for this analysis, we used three-component local waveforms. Earthquake source parameters can then be extracted from a mathematical model, if a good fit is achieved between the measured and synthetic seismograms. The searching process of the highest DC value and its variance reduction to obtain the best seismogram fitting are shown in Figure 3. Double couple (DC) value and its variance reduction for the event are 98.4% and 50%, respectively. The seismogram fitting, DC values, and variance reduction are presented in Figures 2-3. Based on the analysis, source parameters for the main shock are obtained as in Figure 3 and Table 1.

3. Results and Discussion

Station codes (St) and their distance (Δ) used for inversion, and the strike (stk), dip, rake (rak) for the 2009 event are presented in Table 2. Based on the geometrical Dikit segment of the SFZ [1] and [9] and HC method confirmation, we found that the activated fault plane for the mainshock has values of strike=324°, dip=80° and rake=-173°. The accuracy of the focal mechanism estimation can provide vital information regarding the earthquake's strength, orientation, fault plane length, width, slip length and also Coulomb stress changes. The location of the most seismicity lies where the increasing Coulomb stress caused by the mainshocks.

The seismicity we report is consistent with the increasing Coulomb stress that calculated using the

Table 2. Focal Mechanism of the 20091001_01:52:27 Main Shocks

St	Δ(km)	Stk	dip	rak
PDSI	216.97	324°	80°	-173°
RGRI	257.48			
LHSI	261.43			
MDSI	362.74			
LWLI	390.79			
KASI	464.59			
PPBI	511.84			
BLSI	515.88			

activated fault plane parameters (Figure 4). In this research, we used the seismicity catalog from GEOFON, which we revised manually for our specific purpose, and we relocated the events catalog from BMKG.

An examination of Coulomb stress changes induced by the earthquakes that have occurred since 2006 in the Jambi region shows that the entire Dikit segment of the SFZ is located in a region of increasing Coulomb stress, more than 0.02 bar at a depth of 12 km (Figure 4). This plot suggests that up to 90% of Mw>3 shallow earthquakes since 2006 have been located in regions of positive Coulomb stress (red region in Figure 4). In addition to the static stress changes, the dynamic stress changes play an important role in remote triggering, provided that the change is more than ~500 kPa in stress or ~10-6 in strain [15]. This study has significant implications for the seismic hazard assessment of the region, as the change in stress can cause either a delay or an advance in the occurrence of future earthquakes [16]. The Mw=7.9 Denali fault earthquake in 2002 provided enough evidence for the dynamic triggering of earthquakes as far as 3660 km [17]. The further the distance, the more effective is dynamic stress over static stress in triggering earthquakes (Madlazim *et al*., 2010). The aftershocks beyond 2–3 rupture lengths are likely triggered exclusively by post-seismic relaxations of stresses [18].

4. Conclusions

The 1 October 2009 earthquake parameters of the mainshock (moment seismic and moment magnitude parameters), extracted after the fitting between measured and synthetic seismograms and achieved with the best double couple (DC) value and variance reduction of the event, are 98.4% and 50%, respectively. Using the HC method, we obtained that the activated fault plane values for the mainshock are strike=324°, dip=80° and rake= -173°.

Acknowledgements

We would like to express our gratitude to those who helped us finish this research. Thank you to GFZ-Potsdam GEOFON-Germany and BMKG-Indonesia, who gave us permission to download the waveform data recorded by the IA network stations and access to the earthquakes catalog. We also thank Prof. Dr. Jiri Zahradnik and Prof. Dr. Efthimios Sokos, who gave us guidance in understanding ISOLA-GUI and also applying this software to estimate the earthquake source parameters using three-component local waveforms (http://seismo.geology.upatras.gr/isola).

References

[1] D.H. Natawidjaya, Thesis, California Institute of Technology Pasadena, California, 2002.
[2] L. Prawirodirdjo, Y. Bock, R. McCaffrey, J. Genrich, E. Calais, C. Stevens, S.S.O. Puntodewo, C. Subarya, J. Rais, P. Zwick, Fauzi, Geophys. Res. Lett. 24 (1997) 2601.
[3] S. Lasitha, M. Radhakrishna, T.D. Sanu, Current Science, 90/5 (2006) 690.
[4] K.R. Newcomb, W.R. McCann, J. Geophys. Res. 92 (1987) 421.
[5] K. Megawati, T.-C. Pan, Bull. Seismol. Soc. Amer. 99/2A (2009) 566. DOI: 10.1785/0120080109.
[6] P. Goldstein, A. Snoke, SAC Availability for the IRIS Community, DMS Electronic Newsletter, 7/1 (2005) 1. http://www.iris.edu/news/newsletter/vol7 no1/ page1.html, 2005.
[7] E. Sokos, J. Zahradník, Comput. Geosci. 34 (2008) 967.
[8] M. Bouchon, Bull. Seismol. Soc. Amer. 71 (1981) 959.
[9] Madlazim, B.J. Santosa, J.M. Lees, W. Utama, Cent. Eur. J. Geosci. 2/4 (2010) 455. DOI:10.2478/v10085-010-0016-5.
[10] F. Haslinger, E. Kissling, J. Ansorge, D. Hatzfeld, E. Papadimitriou, V. Karakostas, K. Makropoulos, H.-G. Kahle, Y. Peter, Tectonophysics. 304 (1999) 201.
[11] M. Kikuchi, H. Kanamori, Bull. Seismol. Soc. Amer. 81 (1991) 2335.
[12] J. Zahradnik, A. Serpetsidaki, E. Sokos, G.A. Tselentis, Iterative Deconvolution of Regional Waveforms and a Double-event Interpretation of the Lefkada Earthquake, Greece, http://seismo. geology.upatras.gr/isola/, 2006.
[13] O. Coutant, Program of Numerical Simulation AXITRA, Research Report, LGIT, Grenoble, 1989.
[14] J. Zahradnik, F. Gallovic, E. Sokos, A. Serpetsidaki, G.A. Tselentis, Seismol. Res. Lett. 79 (2008) 653.
[15] M. Miyazawa, Geophys. Res. Lett. 38 (2011) L23307, DOI:10.1029/2011GL049795.

[16] Madlazim, B.J. Santosa, W. Utama, Indonesian J. Phys. 21/3 (2010) 71.
[17] S.G. Prejean, D.P. Hill, E.E. Brodsky, S.E. Hough, M.J.S. Johnston, S.D. Malone, D.H. Oppenheimer, A.M. Pitt, K.B. Richards-Dinger, Bull. Seismol. Soc. Amer. 94/6B (2004) S348.
[18] C.D. Reddy, P.S. Sunil, R. Bürgmann, D.V. Chandrasekhar, T. Kato, Natural Hazards 65/2 (2013) 1119. DOI:10.1007/s11069-012-0184-7.